Nat Hazards (2015) 79:1059–1077
DOI 10.1007/s11069-015-1892-6

ORIGINAL PAPER

Flood risk assessment for urban water system in a changing climate using artificial neural network

M. Abdellatif[1] · W. Atherton[1] · R. Alkhaddar[1] · Y. Osman[2]

Received: 14 January 2013 / Accepted: 2 July 2015 / Published online: 21 July 2015

Abstract Changes in rainfall patterns due to climate change are expected to have negative impact on urban drainage systems, causing increase in flow volumes entering the system. In this paper, two emission scenarios for greenhouse concentration have been used, the high (A1FI) and the low (B1). Each scenario was selected for purpose of assessing the impacts on the drainage system. An artificial neural network downscaling technique was used to obtain local-scale future rainfall from three coarse-scale GCMs. An impact assessment was then carried out using the projected local rainfall and a risk assessment methodology to understand and quantify the potential hazard from surface flooding. The case study is a selected urban drainage catchment in northwestern England. The results show that there will be potential increase in the spilling volume from manholes and surcharge in sewers, which would cause a significant number of properties to be affected by flooding.

Keywords Artificial neural network · Climate change · Combined sewer system · Downscaling · Flooding

1 Introduction

Since 1970s, average global temperatures over land have increased by around 0.7 °C. The Intergovernmental Panel on Climate Change (IPCC) projects a future rise of between 0.7 and 1 °C by the end of this century (IPCC 2007a). Changes in precipitation and

✉ M. Abdellatif
m.e.abdellatif@ljmu.ac.uk

[1] Peter Jost Centre, School of the Built Environment, Liverpool John Moores University, Byrom Street, Liverpool L3 3AF, UK

[2] Department of Civil and Built Environment, School of Engineering, Sports and Sciences, University of Bolton, Deane Road, Bolton BL3 5AB, UK

temperature lead to changes in run-off and water availability. Run-off is projected with high confidence to increase by 10–40 % by mid-century at higher latitudes due to increases in rainfall (IPCC 2007b). Climate change increases disaster risk in two ways: firstly, climate change will likely increase the frequency and/or severity of weather and climate hazards. Secondly, climate change will simultaneously increase communities' vulnerability to natural hazards due to combined effects of ecosystem degradation, reduced availability of resources, and changes in peoples' livelihoods (UNISDR 2009).

Statistical downscaling is the most widely used tool in downscaling climate variables from GCMs, which relates large-scale climate variables (predictors) to regional and local variables (predictands) (Wilby et al. 1998). Then, the large-scale output of GCM simulation is fed into this statistical model to estimate the corresponding local and regional climate characteristic (Wilby et al. 2004). Statistical methods assume that the derived relationships between the observed predictors (climate variables) and predictand (i.e., rainfall) will remain constant under conditions of climate change and that the relationships are time invariant (Yarnal et al. 2001 and Fowler et al. 2007).

A number of approaches have been used to downscale the rainfall at small catchment scale for the purpose of climate change impact studies. Linear and nonlinear regression methods have been used extensively to downscale rainfall with the different capabilities of each method highlighted. Beuchat et al. (2012) and Fealy and Sweeney (2007) used generalized linear models (GLMs) to downscale rainfall in Switzerland and Ireland, respectively. The GLM downscaling models developed were found to perform well in reproducing historical rainfall statistics. Muluye (2012) employed the statistical downscaling model (SDSM), ANN, and nearest neighbour-based approaches (KNN) to downscale rainfall in Canada and found that ANN models have greater ability to reproduce historical rainfall. Another study carried out by Hassan and Harun (2012) showed that the SDSM model was highly acceptable in regards to its performance in downscaling daily and annual rainfall in Malaysia. Results from three downscaling methods (multiple linear regressions, multiple nonlinear regression, and stochastic weather generator) have been used by Hashemi et al. (2012) as inputs to obtain improved historical and future rainfall predictions. The results obtained are very encouraging for any future attempts to combine results of multiple statistical downscaling methods. Samadi et al. (2012) used ANNs to determine how future streamflow may change in a semi-arid catchment. Hoai et al. (2011) used a feed-forward multilayer perceptron (MLP) neural network for downscaling precipitation in India and later used the downscaled precipitations as inputs to a rainfall-run-off model for flood prediction. Moreover, Ojha et al. (2010) and Fistikoglu and Okkan (2011) found that ANNs have good performance in downscaling monthly precipitation in India and Turkey, respectively. Several other studies have shown that taking into account the nonlinear nature of the relationships between predictors and the predictand in statistical downscaling models can improve the goodness-of-fit of the model (Huth et al. 2008). Therefore, ANN has been chosen for use in this study.

The pattern of increasing flood damage is repeated worldwide, and concerns persist about the potential for climate change to increase the frequency of flooding in twenty-first century (Doornkamp 1998; Dorland 1999; Smith 1999; Schreider 2000; Frei 2000; Palmer and Räsänen 2002; Milly et al. 2002; Dobler et al. 2012). There are numerous studies that have investigated the impact of climate change on urban flooding. However, most of them were focused on the impacts from rivers and coastal sources, as they are the most apparent and catastrophic in their nature. For England and Wales, the value of assets at risk of river and coastal flooding was estimated at $214 billion in 1998 (Burgess et al. 2000).

Furthermore, urban flooding from drainage systems is another challenge and in the UK; it is estimated to cost £270 million a year in England and Wales with some 80,000 homes are at risk of flooding (Parliamentary Office 2007). Few studies in the UK considered the urban flooding from combined sewer systems. The impacts are expected to increase if no policy changes are made. One of the latest studies, which did consider flooding from combined sewer systems, is the work carried out by the United Kingdom Water Industry Research (UKWIR 2011), which used a weather generator method to generate future rainfall. The study showed that uplifted design storms due to climate change are expected to have a major effect on design of sewer systems, as the current system has been design on historical climate data. Ashley et al. (2006) considers the current state and future pressure on sewer system planning, design, operation, and maintenance in the UK. The study covered periods up to 2020 and from 2020 to 2080 to assess wastewater system performance as a result of climate change. In addition, increase in the extreme rainfall events will lead to excessive increase in the number of spills from combined sewer overflows, which is likely to introduce hazardous substances into receiving waters (Andrés-Doménech et al. 2012; Fitz Gerald 2008; Gamerith et al. 2008). Thus, the design of urban drainage facilities to control flooding needs to take into account the impacts of climate change.

The objective of this study is to improve the understanding of the potential implications of climate change on urban drainage system flood response and introduces an updated methodology and strategy to assess the impacts of climate change on urban drainage infrastructure. Long-term scenarios are required to gain further knowledge of catchment behaviour in order to develop robust and sustainable flood risk management policies for the drainage system. This has been addressed here by using two special report on emissions scenarios (SRES) for the emission of greenhouse gases and three global circulation models (GCMs) to predict future behaviours of a selected urban catchment for the period 2070–2099 (2080s).

2 Wigan drainage catchment and data

The Wigan catchment covers a geographical area in northwest of England (see Fig. 1) around the River Douglas, which extends from Horwich in the northeast to Wigan Wastewater Treatment Works (WWTW) at Hoscar, in the northwest of Wigan. The drainage area drains an area of 5510.09 hectares and serves a residential population of 190, 942. The drainage sewer model of the area has 3813 sub-catchments and a total number of 5569 pipes, which connects 5535 manholes, 98 outfalls, and one storage tank. It has a total run-off surface area of 3953.66 hectares, 76 % of which represents pervious areas and 23 % represents impervious areas. The main receiving water for the wastewater discharges of the drainage areas is the River Douglas and its tributaries. The sewerage network in the study area is made up of a mixture of combined, separate, and partially separate sewers.

Two sets of data have been used in this study. Firstly, an observed daily rainfall data set, collected for Worthington station in the catchment which was obtained from the Environment Agency for England and Wales, for the period 1961–2001. Secondly, the large-scale observed climatic predictors data set was obtained from the National Centre for Environment Predictions (NCEP/NCAR). These data were originally at a resolution of 250 km $\times$ 250 km, but were re-gridded to conform to the output gird of the GCM models. The two sets of data were needed to build the downscaling model for the catchment.

GCM data were obtained from the Canadian Climate Impacts Scenarios Group, for three different GCM models, namely the Hadley Centre (HadCM3) model, the Canadian

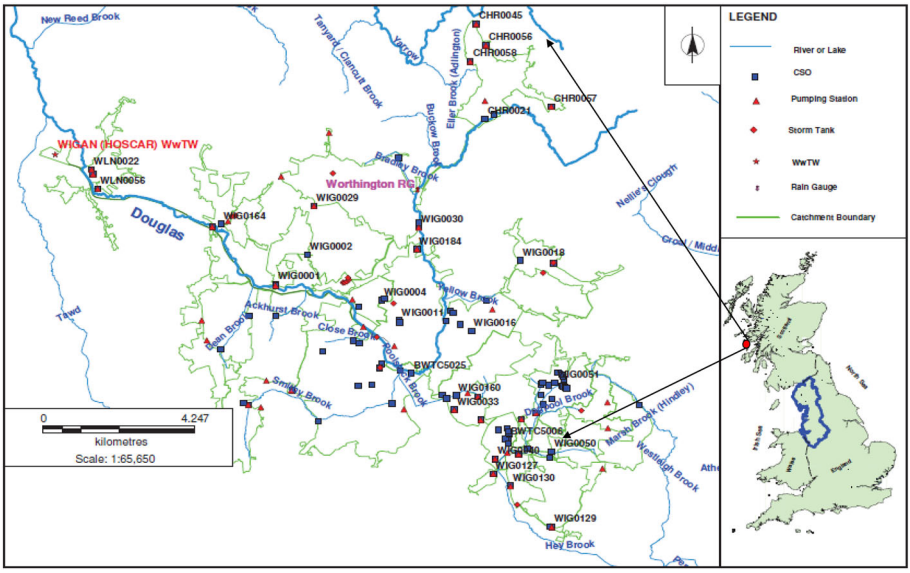

Fig. 1 Wigan drainage area

Centre for Climate Modelling and Analysis (CCCma) (CGCM2) model, and the Commonwealth Scientific and Industrial Research Organization (CSIRO Mark2) model. All the modelled data sets exist on a common grid resolution of 250 km × 357 km, and were obtained for the grid box (the Scottish Border, SB) representing the studied catchment in the GCM domain. The GCM data were obtained for SRES scenarios A1FI, which assumes intensive use of fossil fuel (high CO_2 emission) and B1, which assumes the introduction of efficient and clean technologies (less CO_2 emission).

3 Rainfall model

The methodology for the rainfall downscale model starts with screening for rainfall predictors from very large NCEP climate variables at grid points, followed by constructing the downscale model of the rainfall using the ANN technique to obtain the local-scale future rainfall projection from the coarse-scale GCM variables at gird point. Brief descriptions of how each of these steps has been carried out will be given later in the study.

3.1 Selection of predictors

Selection of suitable climate variable predictors to construct a regression model with the rainfall (predictand) is formed based on correlation coefficients which exist between them. The predictors, which come from NCEP data, are then selected from a range of candidate predictors based on significance and strength of their correlation with the predictand. Stepwise regression has been used to select a sensible combination of predictors from the available data. The stepwise regression is the most sophisticated of the statistical methods used for predictor selection. It usually yields the most powerful and parsimonious model as has been shown in previous studies (Harpham and Wilby 2005). Each variable is entered in

sequence and its contribution to model efficiency is assessed. If adding the variable contributes to the model then it is retained, but all other variables in the model are then re-tested to see whether they are still contributing to the success of the model. If they no longer contribute significantly, then they are removed (Abdellatif et al. 2012). Thus, the method would ensure that the smallest possible set of predictor variables is included in the resulting model (Al-Subaihi 2002; Goyal and Ojha 2010).

3.2 Construction of rainfall model

The current study used an artificial neural network (ANN) as an example of nonlinear regression of statistical downscale methods. The ANN used here is based on a feed-forward configuration of the multilayer perceptron (see Fig. 2) and is composed of multiple simple processing nodes, or neurons, assembled in different layers (input, hidden, output). Each node computes a liner combination of the weighted inputs including a bias term from the links feeding into it. The assumed value of these inputs is transformed using a certain activation function: either linear or nonlinear. The output obtained is then passed as input to other nodes in the following layer. In this study, eight climate variables have been used in the input layer with one node, which is the rainfall, in the output layer. The optimum number of nodes in the hidden layer is determined during the training of the network. Determination of an appropriate number of hidden neurons is important for successful modelling with neural network as the network efficiency is sensitive to this number. If the hidden layer has too few neurons, the network is too parsimonious in its use of parameters, and then, the performance of the ANN may deteriorate below that of the more appropriate number. On the other hand, if the hidden layer has too many neurons, then there are too many parameters and there is a danger of overfitting the training data set with no significant improvement in the training or even a drop in efficiency in the verification period (Master 1993). The appropriate number can be found by training the network and evaluating its performance over a range of different increasing numbers (Hammerstorm 1993) in order to obtain near-maximum efficiency with as few neurons as necessary.

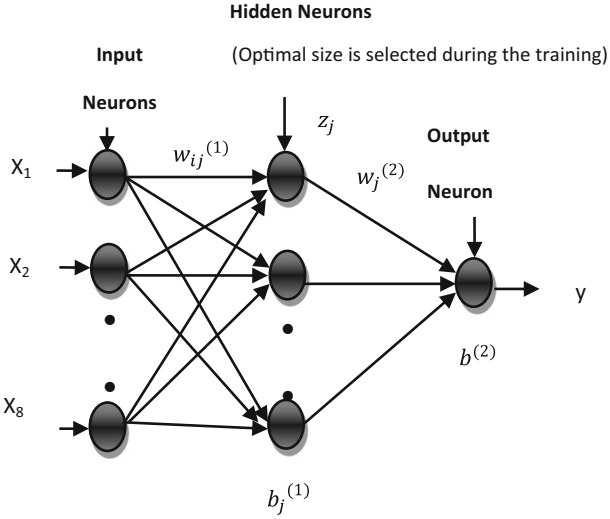

Fig. 2 Feed-forward neural network model

The activation function used in the hidden layer is log-sigmoid and in the output layer is a linear function. The output, y, of the network with eight inputs, k log-sigmoid nodes in the hidden layer, and one linear node in the output layer is given by:

$$y = \sum_{1}^{k} w_j^{(2)} \; z_j + \; b^{(2)} \tag{1}$$

$$z_j = \frac{1}{1 + \exp\left(\sum_1^8 - w_{ij}^{(1)} \; x_i + \; b_j^{(1)}\right)} \tag{2}$$

where x_i corresponds to the ith input, and the coefficients $w_j^{(2)}$ and $b^{(2)}$ ($w_{ij}^{(1)}$ and $b_j^{(1)}$) are the weights and biases from the output (hidden) layers. Z_j is the output from the hidden layer nodes.

ANNs have to be trained in order to obtain best estimates of these weights and biases that can properly associate predictors with the predictand. It is worth mentioning here that biases are much like weights except that they have a constant value of 1, but they are not necessarily to be the in Eqs. (1) and (2), as appropriate trained ANN models can still be obtained if they are omitted. Nevertheless, biases were used here to shift the entire arguments (net input) of activation function to the right or to the left.

The main objective behind an ANN training algorithm is to minimise the mean square error (MSE) (Trigo 2000), in that it is measures the differences between the observed (target) and the predicted (output) n values;

$$\text{MSE} = \frac{1}{n}\left(\sum_{i}^{n} (\text{obs}(i) - \; \text{pred}(i))^2\right) \tag{3}$$

For MLF-ANN, with more than one layer of weightings (as in Figs. 3, 6), the error function will typically be a highly nonlinear function of weightings. Due to this nonlinearity, it is not possible to find an analytical solution for its minimum value. Instead, a numerical algorithm has been sought, which usually involves a search through the weight space consisting of a succession of steps of the form:

$$w_{k+1} = w_k + \nabla w_k \tag{4}$$

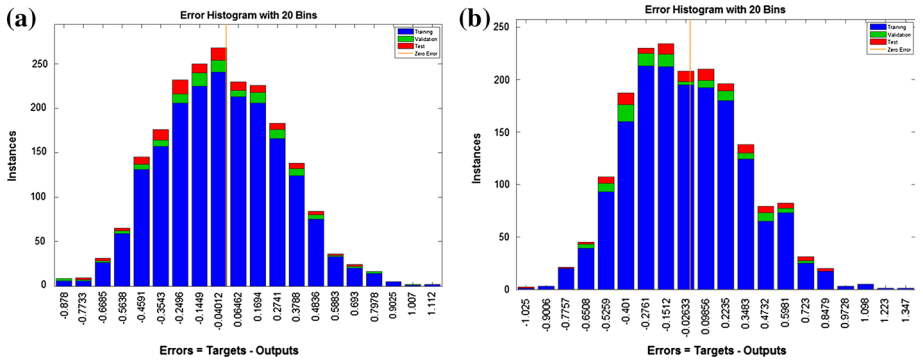

Fig. 3 Histogram of error during training, validation, and test set for **a** winter and **b** summer

where w_{k+1} is the value of a certain weight at a given iteration $k + 1$, w_k is the value of the same weight at previous step k and ∇w is the weight vector increment.

In the present study, an error back-propagation algorithm (Haykin 1994) was employed to obtain a numerical solution for the model parameters using the Levenberg–Marquardt approach (LM). The LM approach, one of the second-order nonlinear optimisation techniques, is usually faster and more reliable than any other back-propagation techniques (Jeong and Kim 2005). The LM method is based on the approximation of the Gauss–Newton method and introduces another approximation to the Hessian matrix, H defined as:

$$H = J^T J + \mu I \tag{5}$$

μ is always positive and called the combination coefficient and I is the identity matrix.

3.3 Evaluation of rainfall model

After calibrating the ANN model, a validation process is always needed to ascertain the accuracy of the future rainfall projection. The validation process enables the model to produce synthetic current daily rainfall data based on inputs of the observed time series data (observed predictors) and the ANN regression parameters produced using independent observed data (obtained from the calibration period). These validation data sets were neglected or reserved during the calibration procedure. In this study, the available daily rainfall from 1961 to 2001 was used for calibration and verification processes. A random process with 90 % of the observed daily rainfall is employed for model calibration with the remaining 5 % used for model validation and another 5 % for model test for each winter (January, February, and December) and summer (June, July, and August) seasons. This division of calibration and validation data comes after many trials in order to get best ANN model with a reasonable performance function.

Performances of the ANN model during calibration and validation were evaluated based on:

1. The correlation coefficient (R), which is defined as,

$$R = \frac{\sum (R_{\text{ob}} - \bar{R}_{\text{ob}})(R_{\text{sim}} - \bar{R}_{\text{sim}})}{\sqrt{\sum (R_{\text{ob}} - \bar{R}_{\text{ob}})^2 \sum (R_{\text{sim}} - \bar{R}_{\text{sim}})^2}} \tag{6}$$

where R_{ob} is the observed rainfall and R_{sim} is the simulated rainfall. $\bar{R}_{\text{ob}}$ and $\bar{R}_{\text{sim}}$ are the mean of observed and simulated rainfall. R is a measure of how well the predicted values from a forecast model fit with the real-life data with a perfect fit giving a coefficient of 1.0.

2. Root mean squared error (RMSE),

$$\text{RMSE} = \sqrt{\frac{\sum_1^N (R_{\text{ob}} - R_{\text{sim}})^2}{N}} \tag{7}$$

where N is the number of observations. Other visual plots to compare the observed and simulated rainfall by the ANN on a seasonal basis are also considered.

The developed ANN model was then used to simulate seasonal future rainfall using a set of input variables generated by global circulation models (for a specific scenario of emission) as predictors (this set of GCM variables corresponds to those of NCEP predictors used in constructing the downscaling model).

4 Elements of the drainage system flow model

A physically deterministic model of sewer flow must represent the inputs (rainfall and wastewater flow) and convert them into information that is needed: flow rate and depth within the system and at its outlets. InfoWorks CS software has been used for the purpose of this simulation. The specific application of this package to the Wigan catchment requires checking, calibration, and verification which has already been completed by the water authorities in Northwest of England. The main components of the flow model are the following:

4.1 Generated wastewater

The constituents of dry weather flow (wastewater) are population-generated flows from residential properties within the network, trade, and commercial flows together with infiltration from groundwater into the sewerage system networks. The Wigan sewer model uses a total population-generated flow of 128 l/h/day and a total trade and commercial flow of 108.24 and 53.6 l/s, respectively. A total annual infiltration flow of 289.38 l/s is used in the model. These total input flows are distributed along the appropriate unit time as dry weather flow generally varies during a day, a week, or a season.

4.2 Rainfall

The model will be used to find responses of the catchment and sewer system to particular rainfall patterns. Sub-daily rainfall of 5 min to 1 h with a particular storm profile (variation of rainfall intensity with time) has been generated for a specific return period using the relationship between intensity, duration, and frequency. This relationship has been achieved through the frequency analysis of the downscaled future rainfall, described in the previous sections, to obtain the design storm using a combined Peak over Threshold-Generalized Pareto Distribution approach (POT-GPD). GPD was introduced by Pickands (1975) and has been applied in a number of fields including reliability studies and analysis of environmental extreme events. The cumulative distributions function for GPD, where $k \neq 0$ is:

$$F(x) = 1 - \left(1 + \frac{k}{\sigma}(x-u)\right)^{-\frac{1}{k}} \tag{8}$$

For $k = 0$ the GPD reduces to an exponential distribution which can be expressed as:

$$F(x) = 1 - \exp\left(\frac{(x-u)}{\sigma}\right) \tag{9}$$

where x is a random variable, $x > u$, with u a threshold, k shape parameter, σ scale parameter.

The Extreme Quantile (X_T) or the design storm estimation for a specified Return Period T is given by:

$$X_T = u + \frac{\sigma}{k}\left[(\lambda T)^k - 1\right] \quad k \neq 0 \tag{10}$$

with lambda (λ) being the average number of extremes per year (($\lambda = m/n$ with m being the total number of extreme in the series and n being the number of years).

Transformation of the rainfall hyetograph into a surface run-off hydrograph involves two principal parts. Firstly, losses due to interception, depression storage, infiltration and evapotranspiration are deducted from the rainfall. The latter generally has an insignificant value in the catchment, which ranges between 1 and 3 mm/day, due to catchment being in the Northwest of England which is characterised by cold weather. Secondly, the resulting effective rainfall can be transformed by surface routing into overland flow (Butler and Davies 2004). In this process, the run-off moves across the surface of the sub-catchment to a nearest entry in the sewerage system where it joins the flow of wastewater at the combined system.

5 Risk assessment methodology

The risk of flooding to properties and basements at low-lying areas is assessed based on the results of surcharge in sewers obtained from the InfoWroks CS model of the catchment for a specific design storm. The methodology followed here is developed by MWH UK Ltd and the built-in in-house software called Data Manager (DM). The authors are permitted to use this software for academic purposes.

The DM main steps to assessing flood risk, due to surcharge to properties and basements, involve:

1. Use of ground model information (digital terrain model or LiDAR) to determine topography of the catchment.
2. Use of a geographical information system to determine locations and addresses of properties and basements in the catchment and levels of floor and basements in each property.
3. Use of a geographical information system to assign properties and basements to a nearest sewer in the catchment model. While it is accepted that not every property will be connected to the nearest link, it will be assumed that all properties are connected for purposes of the flood risk assessment.
4. Assessment of flood risk based on a comparison between the predicted top water level (taken from the InfoWorks CS simulation) and the individual property level. Flood risk to properties is categorised as *VHI—very high impact*—when water level is greater than 200 mm above property level (United Utilities and MWH 2011).

6 Results and discussions

6.1 Rainfall downscale modelling

Correlation coefficients between selected predictors (defined in Table 1) and daily rainfall is presented in Table 2. This combination of predictors has been selected for the ANN model due to their maximum correlation with daily rainfall. The table also reports the partial, zero correlation and p value between the predictors and rainfall that help identify the amount of explanatory power for each predictor. Despite the apparently low correlation coefficient, it was found that these relations are statistically significant at the 5 % level of significance.

Table 1 Predictors definition

Code	Variables
ncepp850+1	Laged forward 850 hpa geopotential height
nceppp8_u	850 hpa zonal velocity
ncepr500	Relative humidity at 500 hpa
nceppp_z(+1)	Laged forward surface vorticity
ncepp_v(+1)	Laged forward surface meridional velocity
ncepp850	850 hpa geopotential height
ncepp_v	surface meridional velocity
ncepp500(+1)	Laged forward 500 hpa geopotential height
ncepp8_z(+1)	Laged forward surface vorticity
ncepmsl(exp)	Exponential for mean sea level pressure
ncepp rhum(+1)	Laged forward near surface relative humidity
ncepp_zh+1	Laged forward surface divergence
ncepr850(+1)	Laged forward relative humidity at 850 hpa
ncepp_zh	Surface divergence

Table 2 Selected large-scale climate variables for winter (top) and summer (bottom) daily rainfall

Predictor	Correlation		
	Zero-order	Partial	*p*
Top			
ncepp850+1	−0.482	−0.078	0.000
ncepp8_u	0.356	0.259	0.000
ncepr500	0.437	0.203	0.000
nceppp_z(+1)	0.459	0.215	0.000
ncepp_v(+1)	−0.080	−0.088	0.000
ncepp850	−0.438	0.068	0.000
ncepp_v	−0.139	−0.530	0.001
ncepp500(+1)	0.246	0.143	0.003
Bottom			
ncepp8_z(+1)	0.530	0.202	0.00
msl (exp)	−0.474	−0.198	0.00
ncepr500	0.333	0.135	0.00
ncepp rhum(+1)	0.436	0.095	0.00
ncepp_v(+1)	−0.163	−0.079	0.00
ncepp_zh+1	−0.138	0.051	0.002
ncepr850(+1)	0.390	0.049	0.003
ncepp_zh	0.101	0.042	0.009

$\alpha = 0.05$ (p should be <0.05 for significant correlation)

Different types of transformation functions are applied for predictors (climate variables) and predictand (rainfall) to improve the correlation coefficient of the regression equation (e.g., Lag+1, fourth root). Generally, eight predictors have been found more suitable in predicting rainfall at the Worthington station to represent the Wigan catchment, according to the higher correlation coefficient of the stepwise regression model.

Table 3 Performance of the downscale model in terms of correlation coefficient, and root mean square error during calibration and verification Stage (1961–2001)

Season	Correlation (*R*)	*RMSE*
Winter	0.78	3.57
Summer	0.69	3.97

The efficiency and ability of each model to predict rainfall amount have been presented using the histogram for training, validation, and the test set error, which show reasonable performance (Fig. 3). Moreover, the generalisation capability of the network that best matched the observed rainfall is expressed in terms of their correlation coefficient (*R*) and root mean square error (RMSE) and is presented in Table 3. The higher values of R and lower values of RMSE obtained by models built using the ANN approach indicate that this modelling approach performed better in the winter than in the summer due to the increased number of wet days which contributes to improvement of model performance.

Additionally, the quantile to quantile plots in Fig. 4 demonstrate the ability of the ANN model to reproduce the daily rainfall in the catchment for the winter and summer seasons. Results from the winter model follow the 45° line very well, as winter extreme rainfall is better represented by the ANN model. For results from the summer model, there is an outlier which could be due to the nature of summer heavy rainfall events, which are normally more intensive than in the winter events. It can also be observed that in both plots, the low amounts of rainfall are better simulated than the high amounts. In general, the model shows reasonable accuracy in reproducing the extreme values, judged here by the closer proximity of the quantile estimate points from the straight diagonal lines.

Figure 5a, b shows the inter-annual variability for the rainfall in the catchment, between the observed and simulated (using NCEP predictors) series for winter and summer in the period 1961–2001 (calibration and verification periods). The average annual values of the simulated rainfall are much closer to the observed ones for both seasons (scatter points are overlaid each other), although the summer model overestimates rainfall in some years. This could be attributed to the nature of extreme rainfall in this season as it is considered more stochastic and intensive compared with the winter extremes. Again, these results demonstrate that the ANN model could be suitable in reproducing the observed rainfall, which is an important requirement when assessing climate impacts on hydrological systems.

The capabilities of the ANN in simulating extreme rainfall were validated by comparing results with the observed extremes for the base period and then subsequently assessed using the impacts of climate change together with projected changes relative to the ANN series. Figure 6 shows an example of the cumulative distribution function for the observed and simulated extreme rainfall in the winter and catchment for winter and summer using GPD. It can be clearly seen in Fig. 6 that the ANN model slightly underestimates the cumulative distribution function for the summer extremes, especially the low values, while the winter model marginally underestimates the low values and overestimates the high extremes.

6.2 Future design storm

The future rainfall for winter and summer seasons has been generated for the future period of the 2080s (2070–2099). Corresponding predictors to those presented in Table 1 were obtained from the HadCM3, CSIRO, and CGCM2 GCMs and used with the calibrated

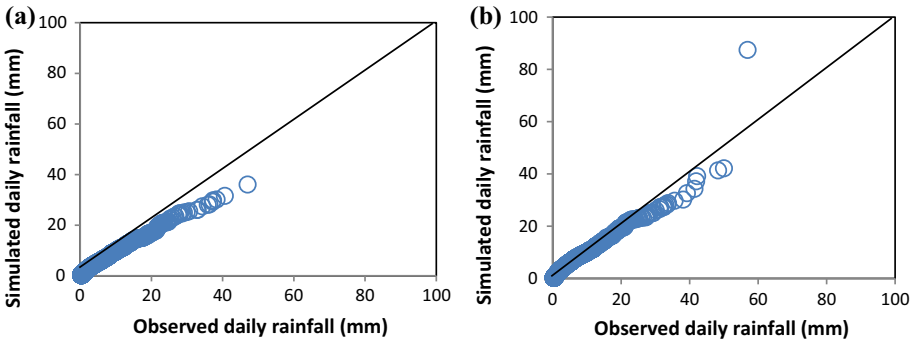

Fig. 4 Quantile–Quantile plot of daily rainfall for year 1961–2001 (calibration and verification period) for **a** winter and **b** summer

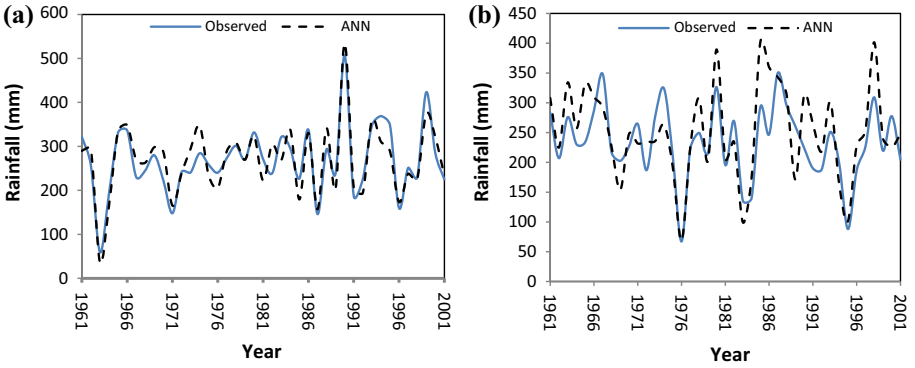

Fig. 5 Inter-annual variability for observed and modelled **a** winter and **b** summer rainfall for Worthington during calibration and verification periods (1961–2001)

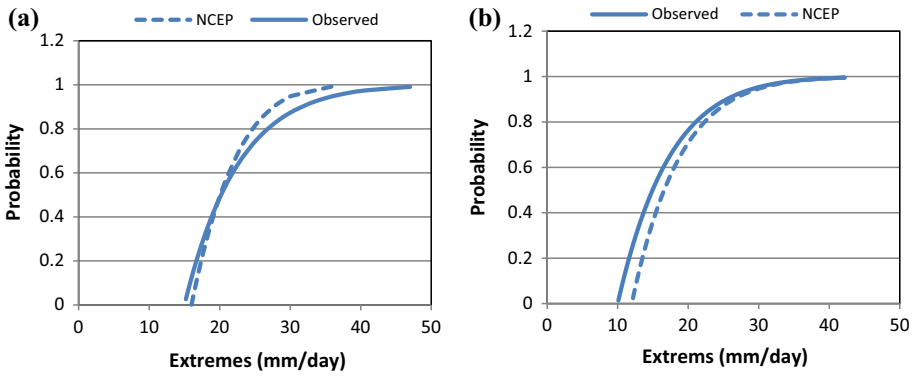

Fig. 6 Cumulative distribution function for observed and NCEP (ANN) extremes for Worthington **a** winter and **b** summer during the base period

ANN downscale model to generate the future rainfall series. Tables 4 and 5 show the uplift factor needed to be used with the current rainfall to estimate the future design storm for different return periods. These uplift factors are obtained from frequency analysis using the POT-GPD approach under A1FI and B1 scenarios. They are calculated by comparing the quantile estimated from the frequency analysis (more details available in Abdellatif et al. 2013) of the future period 2080s rainfall series with that of the base period (1961–1990), as in Table 4 and Fig. 7a, b. It is clear that the catchment in winter is projected to experience an increase in heavy rainfall under the high scenario for return periods up to 30 years of 24-h duration, which has been confirmed by all GCMs. There are differences in the percentage of increase from GCM to another with the HadCM3 showing the maximum increase among the GCMs, ranging between 14 and 21 % for return periods of 2–30 years. For the B1 scenario, the picture is projected to be the opposite. The catchment is anticipated to suffer a pronounced reduction in the design storm.

In Table 5 and Fig. 7c, d, a decrease in the magnitude of return periods for daily design storm in the summer can be noticed. All the GCM models agree that there will be a dramatic decline in the rainfall amount under scenario B1 with the magnitude of this decrease varying between the GCMs. Meanwhile, there will be a jump in rainfall magnitude from the return periods 10–20 and 30 years under scenario A1FI, indicating a slight increase in daily design storm for the HadCM3 GCM. The patterns of these design storms are represented in Fig. 7 for winter and summer under A1F and B1, compared with the control period, and were generated for up to 30-year return period.

6.3 Combined sewers system modelling

The aim is to study climate change impacts on the future behaviour of the hydrological system of the Wigan drainage area in Northwest England for the future period of the 2080s. The impacts will be assessed based on the change in manhole flood volumes, surcharge in sewers, and the number of buildings at risk of flooding. Design storms for return periods 2, 5, and 10 years in the future period of the 2080s will be used for this purpose.

The number of manholes in the Wigan drainage area, where water level exceeds the ground level, is predicted to increase in the winter seasons of the future period under scenario A1FI as predicted by the three GCMs. For example, the HadCHM3 GCM projects a number of flooding manholes of 210 compared to 156 manholes predicted during the baseline period for a 2-year 1440-min design storm. Subsequently, the total flood volume is projected to increase to a maximum of 1.4, 1.5, and 1.9 times the current situation for return periods 2, 5, and 30 years, respectively. This is due to an increase of 14, 15, and 28 % in the design storm, as predicted by the HadCM3 and CGCM2 GCMs (Tables 4 and

Table 4 Uplift factors for Wigan winter in 2080s for the three GCMs under AIFI and B1

Return period (years)	A1FI scenario			B1 scenario		
	HadCM3	CSIRO	CGCM2	HadCM3	CSIRO	CGCM2
2	1.14	1.09	1.05	0.83	0.72	0.70
5	1.15	1.06	1.09	0.84	0.77	0.68
10	1.17	1.05	1.14	0.86	0.82	0.68
20	1.19	1.04	1.22	0.89	0.89	0.68
30	1.21	1.04	1.28	0.91	0.94	0.68

Table 5 Uplift factors for Wigan summer in 2080s for the three GCMs under AIFI and B1

Return period (years)	A1FI scenario			B1 scenario		
	HadCM3	CSIRO	CGCM2	HadCM3	CSIRO	CGCM2
2	0.77	0.71	0.96	0.53	0.58	0.63
5	0.85	0.74	0.94	0.56	0.58	0.64
10	0.93	0.78	0.93	0.61	0.58	0.66
20	1.02	0.81	0.91	0.67	0.59	0.67
30	1.08	0.84	0.90	0.71	0.59	0.68

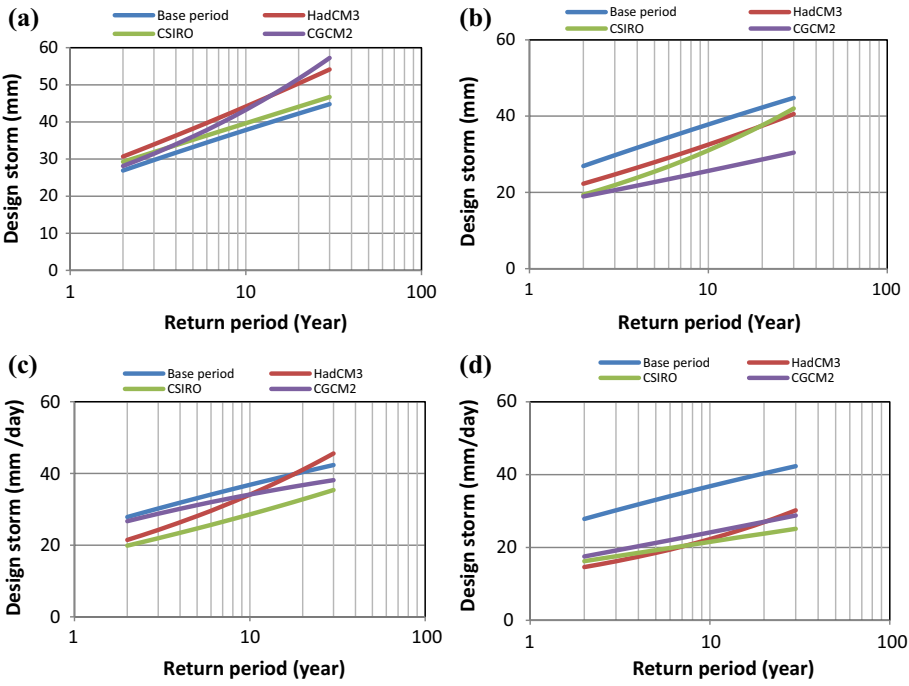

Fig. 7 Design storm–return period relationship for winter **a** AIFI, **b** B1 and summer **c** AIFI, **d** B1

6). However, under the low scenario B1, a slight decrease in the total flood volume from manholes is projected by the three GCMs.

For the summer seasons of the future period and under both scenarios, the total flood volume from the manholes is projected to reduce, especially under scenario B1 due to the expected decrease in the greenhouse emissions (Tables 5 and 7).

The geographical distribution of the flooding in the catchment can vary with the spreading of the flooded manholes; it is much wider in the future period under the winter of the AFI scenario compared to the baseline period (Fig. 8). In Fig. 8, the number of flooding manholes is predicted to increase by 34 %, and the corresponding total flood volume, from these manholes, is only 23 % higher than the total flood volume in the base period for a

Table 6 Consequences of climate change on the drainage system in Wigan winter in terms of surface flooding and number of surcharged sewers

Consequence	A1FI scenario				B1 scenario		
	Current	HadCM3	CSIRO	CGCM2	HadCM3	CSIRO	CGCM2
$T = 2$ years: surface flooding (million m^3)	0.061	0.087	0.078	0.070	0.035	0.023	0.021
Surcharged sewers	475	586	548	511	364	307	293
$T = 5$ years: surface flooding (million m^3)	0.106	0.153	0.125	0.135	0.067	0.051	0.034
Surcharged sewers	634	771	690	719	494	446	367
$T = 30$ years: surface flooding (million m^3)	0.304	0.504	0.339	0.587	0.234	0.256	0.108
Surcharged sewers	1082	1358	1145	1443	956	996	641

2-year 1440-min design storm, as simulated by the HadCM3 GCM. This indicates that the relationship between the cause of flooding and its consequences is nonlinear.

The increase in design storm intensity in winter under scenario A1FI indicates that there might be more damage to properties due to surcharged sewers when the hydraulic gradient is increased above the property floor or basement levels as shown in Figs. 9 and 10. In the winter seasons, under scenario B1, and the summer seasons under both scenarios, a drop in the number of surcharged sewers is predicted, and consequently the number of properties at risk of flooding will decrease as a result of this. This has been reflected in the results in Tables 6 and 7 and demonstrated in Fig. 9.

The findings presented in this paper reflect the potential risk and opportunities and does not give a definite answer of what the future consequences of climate change will be. This is due to uncertainties over the magnitude and timing of climate change impacts, especially at regional and local levels. This is partly because of GCMs limitations and inability to model the climate system, biophysical impacts, and the social and economic responses to changes in climate (CCRA 2012). Despite these uncertainties related to future climate

Table 7 Consequences of climate change on the drainage system in Worthington summer in terms of surface flooding and number of surcharged sewers

Consequence	A1FI scenario				B1 scenario		
	Current	HadCM3	CSIRO	CGCM2	HadCM3	CSIRO	CGCM2
$T = 2$ years: surface flooding (million m^3)	0.052	0.026	0.020	0.046	0.013	0.012	0.014
Surcharged sewers	551	422	367	526	295	289	307
$T = 5$ years: surface flooding (million m^3)	0.093	0.058	0.039	0.078	0.024	0.020	0.025
Surcharged sewers	730	581	483	678	412	379	413
$T = 30$ years: surface flooding (million m^3)	0.272	0.251	0.173	0.204	0.122	0.066	0.096
Surcharged sewers	1224	1173	982	1069	820	621	744

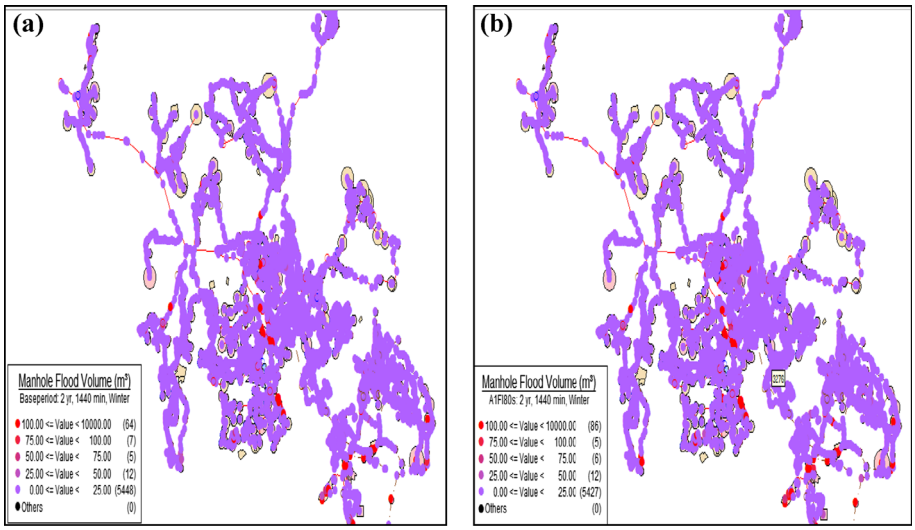

Fig. 8 Location of flooding manholes in Wigan catchment in **a** the present and **b** future under scenario A1FI 2080s (2070–2099); in winter due to 2-year 1440-min storm where the number of total flooding manholes is 156 and 210, respectively, as simulated by HadCM3

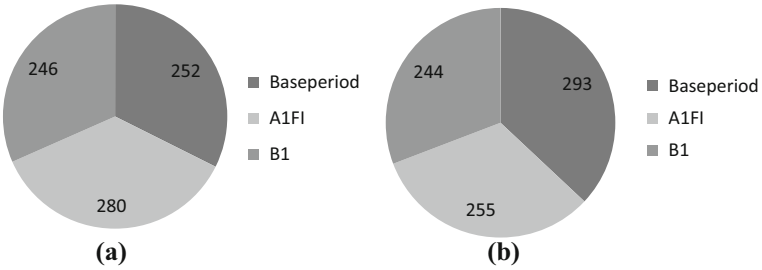

Fig. 9 Number of properties at very high risk of flooding due surcharged sewers for storm 5-year return period for winter (**a**) and summer (**b**) simulated using HadCM3

change and its impacts, the fact that the climate change has already started is sufficient evidence for the outcome of the impact studies. Thus, it is possible to identify a range of possible outcomes that can inform adaptation policies and planning.

7 Conclusions

Climate change is one of the main challenges to urban drainage systems in the future decades. As such, this challenge receives a lot of attention, with a general approach of model-based analysis of impacts of singular climate changes, e.g., the impact of more intense storm events in summer or of prolonged wet periods in winter.

This paper presents results of a downscaling methodology for assessment of impacts of climate change on an urban drainage system. The results explained variability in design

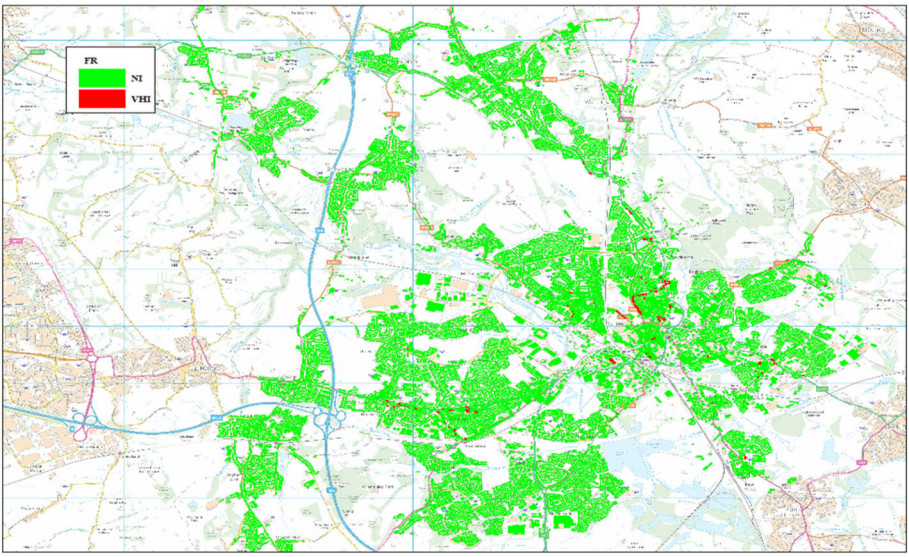

Fig. 10 Location of 400 properties at very high risk of flooding (*red dots*) out of 88,842 totals at Wigan catchment due to surcharged sewers in winter of 2080s (2070–2099) under AFI for storm of 5-year return period, 24-h duration simulated using HadCM3. *NI* no impact, *VHI* very high impact

rainfall extends to the end of the current century. Results also highlight examples of increase in flood volume from manholes, which is likely to cause more surfaces flooding in the future during winter periods at A1FI scenarios only. Hence, the number of basements at risk of flooding will also increase. Conversely summer period for both scenarios and winter under B1 suffer from some reduction in the design storm causing low surface flood risk.

Acknowledgments This paper is part of a research project conducted at Liverpool John Moores University in collaboration with MWH UK Ltd and United Utilities Plc in Northwest England. The authors would like to extend their thanks to Innovyze UK, for providing the InforWorks CS license. The views expressed in the paper are those of the authors and not necessarily those of the collaborating bodies.

References

Abdellatif M, Atherton W, Alkhaddar R (2012) Climate change impacts on the extreme rainfall for selected sites in North Western England. Open J Mod Hydrol 2(3):49–58

Abdellatif M, Atherton W, Alkhaddar R (2013) A hybrid generalised linear and Levenberg–Marquardt ANN approach for downscaling future rainfall. Hydrol Res J 44(6):1084–1101

Al-Subaihi AA (2002) Variable selection in multivariable regression using SAS/IML. J Stat Softw 7(12):1–20

Andrés-Doménech I, Montanari A, Marco J (2012) Efficiency of storm detention tanks for urban drainage systems under climate variability. J Water Resour Plann Manage 138(1):36–46. doi:10.1061/(ASCE)WR.1943-5452.0000144

Ashley R, Tait S, Cashman A, Blanksby J, Hurley AL, Sandlands L, Saul A (2006) 21st sewerage design; full report, UKWIR Report 06/WM07/7

Beuchat X, Schaefli B, Soutter M, Mermoud A (2012) A robust framework for probabilistic precipitations downscaling from an ensemble of climate predictions applied to Switzerland. J Geophys Res 117(D14):1984–2012

Burgess K, Deakin R, Samuels P, Chatterton J, Penning-Rowsell E (2000) Assessment of economic value of national assets at risk from flooding and coastal erosion. In: Proceedings of the DEFRA conference of river and coastal and engineers, pp 04.3.1–04.3.10, UK. MAFF
Butler D, Davies J (2004) Urban drainage. Spon press, USA and Canada
Climate Change Risk Assessment (CCRA) (2012) Summary of key findings from the UK climate change risk assessment 2012
Dobler C, Bürger G, Stötter J (2012) Assessment of climate change impacts on flood hazard potential in the Alpine Lech watershed. J Hydrol 460–461:29–39
Doornkamp JC (1998) Coastal flooding, global warming and environmental management. J Environ Manage 52:327–333
Dorland C (1999) Vulnerability of the Netherlands and Northwest Europe to storm damage under climate change. Clim Change 43(3):513–535
Fealy R, Sweeney J (2007) Statistical downscaling of precipitation for selection of sites in Ireland employing a generalised linear modelling approach. Int J Climatol 27(15):2083–2094
Fistikoglu O, Okkan U (2011) Statistical downscaling of monthly precipitation using NCEP/NCAR reanalysis data for Tahtali River Basin in Turkey. J Hydrol Eng 16(2):157–164
Fitz Gerald A (2008) Financial impacts of sporadic pollution events, Report for Shellfish Association of Great Britain
Fowler HJ, Blenkinsop S, Tebaldi C (2007) linking climate change modelling to impacts studies: recent advances in downscaling techniques for hydrological modelling. Int J Clim 27:1547–1578
Frei C (2000) Climate dynamics and extreme precipitation in flood events in Central Europe. Integr Assess 1(4):281–300
Frei C et al (2006) Future change of precipitation extremes in Europe: intercomparison of scenarios from regional climate models. J Geophys Res 111:D06105. doi:10.1029/2005JD005965
Gamerith V, Olsson J, Camhy D, Hochedlinger M, Kutschera P, Schlobinski S, Gruber1 G, Gruber1 G (2008) Assessment of combined sewer overflows under climate change urban drainage pilot study linz. In: World congress on water, climate and energy conference, Dublin
Goyal MK, Ojha CH (2010) Evaluation of various linear regression methods for downscaling of mean monthly precipitation in Arid Pichola Watershed. Nat Resour 1:11–18
Hammerstorm D (1993) Working with neural networks. In: IEEE spectrum, pp 46–53
Harpham C, Wilby RL (2005) Multisite-downscaling of heavy daily precipitation occurrence and amounts. J Hydrol 312:1–21
Hashemi MZ, Shamseldin YA, Melville BW (2012) Statistically downscaled probabilistic multi-model ensemble projections of precipitation change in a watershed. Hydrol Process 27(7):1021–1032
Hassan Z, Harun S (2012) Application of statistical downscaling model for long lead rainfall prediction in Kurau River catchment of Malaysia. Malays J Civil Eng 24(1):1–12
Haykin S (1994) Neural networks: a comprehensive foundation. MacMillan, New York
Hoai ND, Udo K, Mano A (2011) Downscaling global weather forecast outputs using ANN for flood prediction. J Appl Math. doi:10.1155/2011/246286
Huth R, Kliegrova S, Metelka L (2008) Non-linearity in statistical downscaling: does it bring an improvement for daily temperature in Europe? Int J Climatol 28(4):465–477
IPCC (2007a) Climate change 2007. The physical science basis IPCC working group II contribution of working group I to the fourth assessment report of the intergovernmental panel on climate change. In: Solomon S, Qin D (eds)
IPCC (2007b) Summary for policymakers. In: Parry ML, Canziani OF, Palutikof JP, van der Linden PJ, Hanson CE (eds) Climate Change 2007: Impacts, adaptation and vulnerability. Contribution of working group II to the fourth assessment report of the intergovernmental panel on climate change, Cambridge University Press, Cambridge, pp 7–22
Jeong D-I, Kim Y-O (2005) Rainfall-runoff models using artificial neural networks for ensemble stream flow prediction. Hydrol Process 19(19):3819–3835. doi:10.1002/hyp.5983
Master T (1993) Practical neural networks recipes in C ++. Academic Press Inc, San Diego, p 51
Milly PCD, Wetherald RT, Dunne KA, Delworth TL (2002) Increasing risk of great floods in a changing climate. Nature 415:514–517
Muluye GY (2012) Comparison of Statistical Methods for Downscaling Daily Precipitation. J Hydroinf 14(4):1006–1023
Ojha CSP, Goyal MK, Adeloye AJ (2010) Downscaling of precipitation for lake catchment in arid region in India using linear multiple regression and neural networks. Open Hydrol J 4:122–136
Palmer TN, Räsänen J (2002) Quantifying the risk of extreme seasonal precipitation events in a changing climate. Nature 415:512–514
Parliamentary Office of Science and Technology (2007) Report number 289. Urban flooding

Pickands J (1975) Statistical inference using extreme order statistics. Ann Stat 3:119–131
Samadi S, Carbone GJ, Mahdavi M, Sharifi F, Bihamta MR (2012) Statistical downscaling of climate data to estimate streamflow in a semi-arid catchment. Hydrol Earth Syst Sci Discuss 9(4):4869–4918
Schreider SY (2000) Climate change impacts on urban flooding. Clim Change 47(1):91–115
Smith DI (1999) Urban flood damage and greenhouse scenarios—the implications for policy: an example from Australia. Mitig Adapt Strateg Global Change 4(3):331–342
Trigo RM (2000) Improving metrological downscaling methods with artificial neural network models. Dissertation, University of East Anglia
UKWIR (2011) Climate Change Modelling for Sewerage Networks. Report published by UKWIR Limited, London
United Nations International Strategy for Disaster Reduction Secretariat (UNISDR) (2009) Global assessment report on disaster risk reduction, http://www.unisdr.org/eng/risk-reduction/climate-change/climate-change.html
United Utilities and MWH (2011) Flood risk methodology, AMP5 Model Maintence. Unpublished. Users Guide notes for MWH Engineers. Warrington
Wilby RL, Wigley TML, Conway D, Jones PD, Hewitson BC, Main J, Wilks DS (1998) Statistical downscaling of generation circulation model output: a comparison of methods. Water Resour Res 34:2995–3008
Wilby RL, Charles SP, Zorita E, Timbal B, Whetton P, Mearns LO (2004) Guideline for use of climate scenarios development from statistical downscaling methods. Environmental agency, King College London, CSIRO land and water, GKSS, Bureau of Meteorology. CSIRO atmospheric research and National centre for atmospheric research
Yarnal B, Comrie A, Frakes B, Brown D (2001) Developments and prospects in synoptic climatology. Int J Climatol 21:1923–1950